Epistasis and Allele Specificity in the Emergence of a Stable Polymorphism in *Escherichia coli*

inserted into membranes (Fig. 1, B and C, and fig. S8).

In agreement with the 1:1 stoichiometry of the TSPO-PK11195 interaction (11), only a single set of protein-ligand contacts was observed (Fig. 2A and table S1). Sixty-one contacts of PK11195 to TSPO described a binding pocket formed by the five transmembrane helices in the upper cytosolic part of the helical bundle (Fig. 2, B and C). PK11195 binds to mTSPO with the E-amide rotamer (Fig. 2, A and B), although free in solution both the E- and Z-rotameric conformations are possible (24). PK11195 contacts several conserved residues in the binding pocket that is formed by residues Ala^{23}, Val^{26}, Leu^{49}, Ala^{50}, Ile^{52}, Trp^{107}, Ala^{110}, Leu^{114}, Ala^{147}, and Leu^{150} (Fig. 2, B and C, and fig. S7). One of these residues, Ala^{147}, is particularly interesting, as its natural polymorphism to threonine (Ala^{147} → Thr polymorphism, rs6971) strongly affects TSPO binding of second-generation radioligands—but not PK11195—and thereby the application of these ligands in humans (25). The binding pocket is closed from the cytosolic side by the long loop between TM1 and TM2 (Fig. 1, A and B, and fig. S7). Deletion of residues 41 to 51 in mTSPO as well as site-directed mutagenesis in several species supported the importance of the TM1-TM2 loop for PK11195 binding (19, 26). The mode of PK11195-TSPO binding is likely to be important for other interactions, as PK11195 competes with several small molecules for binding to TSPO (1, 2, 10). In addition, synthetic or endogenous ligands might involve additional binding sites (1, 2, 10), providing a further level of regulation of TSPO function.

Cholesterol binds with nanomolar affinity to recombinant TSPO (11). The interaction occurs through the cholesterol recognition sequence (residues 147 to 159; Ala-Thr-Val-Leu-Asn-Tyr-Tyr-Val-Trp-Arg-Asp-Asn-Ser) at the C terminus of TM5 (Fig. 3A) (19, 27). The 3D structure of the TSPO-PK11195 complex reveals that the side chains of Tyr^{152}, Tyr^{153}, and Arg^{156}, which are essential for cholesterol binding (19, 27), are located on the outside of the TSPO structure and point toward the membrane environment (Fig. 3B). They are therefore not involved in binding to PK11195, consistent with the finding that site-directed mutagenesis of these residues inhibited binding to cholesterol but not to PK11195 (19, 27). The location of residues essential for cholesterol binding at the outside of the TSPO structure, in combination with the known ability of cholesterol to dimerize, suggests that cholesterol binding can modulate the oligomerization of TSPO. Indeed, several transporters function as dimers (28). Residues from the cholesterol recognition sequence, as well as Leu^{112} to Val^{115} in TM4, are highly stable, as evidenced by hydrogen-deuterium exchange (Fig. 3C and fig. S9). Thus, binding of PK11195 stabilizes the 3D structure of TSPO, in agreement with the pronounced increase in NMR signal dispersion upon addition of PK11195 (fig. S1). The ligand-induced stabilization of the TSPO structure might provide

a mechanism to promote transport of cholesterol (Fig. 3A) (12, 13), consistent with the observation that PK11195 markedly increased the binding of cholesterol to TSPO polymers (23).

The 3D structure of the TSPO-PK11195 complex reveals how the members of this important receptor family are organized at the molecular level and provides a basis for understanding the function of TSPO in physiological and pathological conditions.

References and Notes

1. V. Papadopoulos et al., Trends Pharmacol. Sci. 27, 402–409 (2006).
2. R. Rupprecht et al., Nat. Rev. Drug Discov. 9, 971–988 (2010).
3. J. Fan, P. Lindemann, M. G. Feuilloley, V. Papadopoulos, Curr. Mol. Med. 12, 369–386 (2012).
4. C. Braestrup, R. F. Squires, Proc. Natl. Acad. Sci. U.S.A. 74, 3805–3809 (1977).
5. L. Veenman, V. Papadopoulos, M. Gavish, Curr. Pharm. Des. 13, 2385–2405 (2007).
6. L. Veenman, M. Gavish, Curr. Mol. Med. 12, 398–412 (2012).
7. W. Frank et al., Plant J. 51, 1004–1018 (2007).
8. A. M. Scarf, L. M. Ittner, M. Kassiou, J. Med. Chem. 52, 581–592 (2009).
9. R. Rupprecht et al., Science 325, 490–493 (2009).
10. D. R. Owen, P. M. Matthews, Int. Rev. Neurobiol. 101, 19–39 (2011).
11. J. J. Lacapère et al., Biochem. Biophys. Res. Commun. 284, 536–541 (2001).
12. K. E. Krueger, V. Papadopoulos, J. Biol. Chem. 265, 15015–15022 (1990).
13. V. Papadopoulos, A. G. Mukhin, E. Costa, K. E. Krueger, J. Biol. Chem. 265, 3772–3779 (1990).
14. A. M. Barron et al., J. Neurosci. 33, 8891–8897 (2013).
15. J. Gatliff, M. Campanella, Curr. Mol. Med. 12, 356–368 (2012).
16. E. Joseph-Liauzun, P. Delmas, D. Shire, P. Ferrara, J. Biol. Chem. 273, 2146–2152 (1998).
17. S. Murail et al., Biochim. Biophys. Acta 1778, 1375–1381 (2008).
18. V. M. Korkhov, C. Sachse, J. M. Short, C. G. Tate, Structure 18, 677–687 (2010).
19. H. Li, V. Papadopoulos, Endocrinology 139, 4991–4997 (1998).
20. F. Shah, S. P. Hume, V. W. Pike, S. Ashworth, J. McDermott, Nucl. Med. Biol. 21, 573–581 (1994).
21. See supplementary materials on Science Online.
22. J. Liu, M. B. Rone, V. Papadopoulos, J. Biol. Chem. 281, 38879–38893 (2006).
23. F. Delavoie et al., Biochemistry 42, 4506–4519 (2003).
24. Y. S. Lee, F. G. Siméon, E. Briard, V. W. Pike, ACS Chem. Neurosci. 3, 325–335 (2012).
25. D. R. Owen et al., J. Nucl. Med. 52, 24–32 (2011).
26. R. Farges et al., Mol. Pharmacol. 46, 1160–1167 (1994).
27. N. Jamin et al., Mol. Endocrinol. 19, 588–594 (2005).
28. E. A. Morrison, K. A. Henzler-Wildman, Biochim. Biophys. Acta 1818, 814–820 (2012).

Epistasis and Allele Specificity in the Emergence of a Stable Polymorphism in *Escherichia coli*

Jessica Plucain,[1,2] Thomas Hindré,[1,2] Mickaël Le Gac,[1,2*] Olivier Tenaillon,[3,4] Stéphane Cruveiller,[5,6] Claudine Médigue,[5,6] Nicholas Leiby,[7,8] William R. Harcombe,[7†] Christopher J. Marx,[7,9‡] Richard E. Lenski,[10,11] Dominique Schneider[1,2§]

Ecological opportunities promote population divergence into coexisting lineages. However, the genetic mechanisms that enable new lineages to exploit these opportunities are poorly understood except in cases of single mutations. We examined how two *Escherichia coli* lineages diverged from their common ancestor at the outset of a long-term coexistence. By sequencing genomes and reconstructing the genetic history of one lineage, we showed that three mutations together were sufficient to produce the frequency-dependent fitness effects that allowed this lineage to invade and stably coexist with the other. These mutations all affected regulatory genes and collectively caused substantial metabolic changes. Moreover, the particular derived alleles were critical for the initial divergence and invasion, indicating that the establishment of this polymorphism depended on specific epistatic interactions.

Heritable differences in ecologically important traits can allow distinct lineages to arise and coexist. In sexual organisms, divergence typically occurs when populations are geographically separated, and the lineages may or may not persist in the event of later contact (1, 2). In asexual organisms, divergent lineages can arise and persist even in sympatry if ecological opportunities are available (3–7). Divergent lineages have been seen to evolve in environments with unexploited resources (4, 6) or spatial gradients (3); these opportunities are sometimes generated by the organisms themselves through secretion of metabolites (5, 7) and other forms

of niche construction (8). Selective processes, including character displacement and trade-offs in life-history traits or metabolic functions, can promote divergence by causing negative frequency-dependent interactions between nascent lineages (1–7, 9). However, the genetic changes necessary to construct an ecologically distinct lineage are incompletely understood except when they involve single mutations (3, 5). Genome sequencing identified all of the mutations fixed during episodes of divergence in two earlier studies (10, 11) where multiple resources were exogenously provided, although the precise sets of mutations required for coexistence were not fully elucidated.
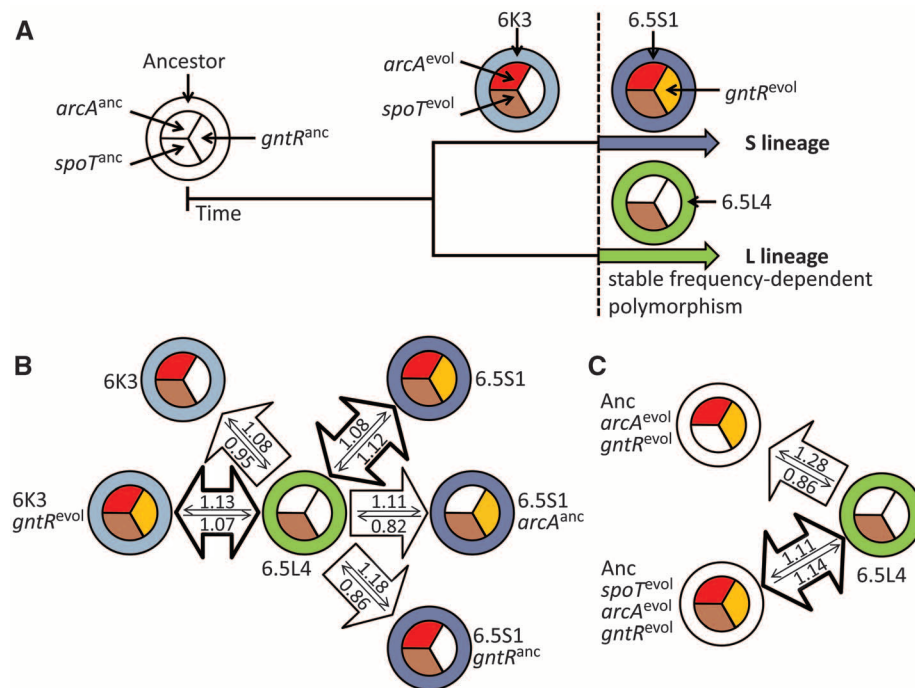
Here, we identify three mutations that together allow one bacterial lineage to invade and stably coexist with another (7, 12–14). Twelve populations were founded from the same strain of *Escherichia coli* and propagated in a glucose-limited minimal medium for >50,000 generations (15, 16). In the Ara–2 population, two lineages, S and L, diverged by 6500 generations and coexist thereafter (7, 12–14). Their coexistence involves niche construction through cross-feeding; the L ecotype grows faster on glucose but secretes by-products that S can better exploit, generating negative frequency-dependent selection. Global transcription profiling identified functional changes specific to the S lineage that appear to be important for its emergence and maintenance (14), but the mutations that caused those differences were not identified, nor were any specific differences shown to play a causal role. We sequenced the genomes of two clones sampled at 6500 generations from each lineage (17): 6.5S1, 6.5S2, 6.5L4, and 6.5L9. We identified candidate alleles and moved them between genetic backgrounds to investigate how the S type invaded and established a persistent lineage.

These clones average 199 mutations compared with the ancestor (18) (table S1); this population became hypermutable when a mutation affecting mismatch repair was fixed early in the experiment (19). Sixty-eight mutations were shared by all four clones (fig. S1 and table S2), implying that they occurred before the S and L lineages diverged. Fifty-five mutations were specific to the S clones and 36 to the L clones (tables S3 and S4). From these data, we estimate that the lineages split between generations 3500 and 4000 (17). However, the phenotypic differences that allowed coexistence arose later. Given hundreds of mutations, it was impossible to manipulate them all. Instead, we sought to identify a minimal set sufficient to allow the S type to invade and stably coexist with the L type. We reasoned that these conditions would require both S-specific mutations and beneficial mutations that arose before the S and L lineages diverged, by which time substantial fitness gains had already accrued (15).

We scrutinized the S- and L-specific mutations based on the lineage-specific differences in gene expression (14). Two S-specific mutations affected the *arcA* and *gntR* genes, which encode regulators of the TCA cycle and the Entner-

Doudoroff pathway, respectively (20, 21). We found both mutations in all S clones from 6500 generations onward, whereas at 6000 generations only the *arcA* allele was present, indicating that it arose before the *gntR* allele (Fig. 1A). We constructed a set of isogenic strains except for the *arcA* and *gntR* alleles in the ancestral and 6.5S1 backgrounds (17). We competed these strains against 6.5L4 using a reciprocal-invasion design (17) that allowed us to distinguish frequency-dependent and generic fitness effects. With both its derived *arcA* and *gntR* alleles, the 6.5S1 clone could invade 6.5L4, but it could not invade if either allele was replaced by the ancestral form (Fig. 1B and fig. S2A). Also, moving the *gntR* allele into a 6000-generation "pre-S" clone (6K3) that carried the *arcA* allele gave the ability to invade 6.5L4 (Fig. 1B and fig. S2B). Thus, the derived *arcA* and *gntR* alleles both contributed to establishing the S lineage.

When these *arcA* and *gntR* alleles were moved alone or together into the ancestral background, they did not allow invasion of 6.5L4 (Fig. 1C and fig. S3), although together they improved fitness by ~10% when rare (fig. S3), indicating ecological differentiation from the L lineage. However,

[1]Laboratoire Adaptation et Pathogénie des Microorganismes, Université Joseph Fourier, Institut Jean Roget, F-38041 Grenoble, France. [2]CNRS UMR5163, F-38041 Grenoble, France. [3]INSERM, Infection Antimicrobials Modelling Evolution (IAME), UMR 1137, F-75018 Paris, France. [4]Université Paris Diderot, IAME, UMR 1137, Sorbonne Paris Cité, F-75018 Paris, France. [5]CNRS-UMR 8030, 91057 Evry Cedex, France. [6]CEA/DSV/IG/ (Commissariat à l'Energie Atomique et aux Energies Alternatives/Direction des Sciences du Vivant/Institut de Génomique) Genoscope LABGeM (Laboratoire d'Analyses Bioinformatiques en Génomique et Métabolisme), 91057 Evry Cedex, France. [7]Department of Organismic and Evolutionary Biology, Harvard University, Cambridge, MA 02138, USA. [8]Systems Biology Program, Harvard University, Cambridge, MA 02138, USA. [9]Faculty of Arts and Sciences, Center for Systems Biology, Harvard University, Cambridge, MA 02138, USA. [10]Department of Microbiology and Molecular Genetics, Michigan State University, East Lansing, MI 48824, USA. [11]BEACON Center for the Study of Evolution in Action, Michigan State University, East Lansing, MI 48824, USA.

*Present address: Ifremer Dyneco/Pelagos, 29280 Plouzane, France.

†Present address: Department of Ecology, Evolution and Behavior, University of Minnesota Twin Cities, St. Paul, MN 55108, USA.

‡Present address: Department of Biological Sciences, University of Idaho, Moscow, ID 83844, USA.

§Corresponding author. E-mail: dominique.schneider@ujf-grenoble.fr

Fig. 1. Effects of focal mutations on ability of S to invade and coexist with L. (**A**) Genotypes are shown as circles, with outer rings denoting genetic backgrounds (white and colors for ancestral and evolved, respectively). The three sectors in each circle show the ancestral (anc, white) or experimentally evolved (evol, colors), i.e., derived, status for each of the *spoT*, *arcA*, and *gntR* genes. (**B**) Clones sampled at 6000 or 6500 generations and modified strains with different *arcA* or *gntR* alleles competed against clone 6.5L4. (**C**) Modified ancestral strains with derived *arcA* and *gntR* alleles and either ancestral or derived *spoT* allele competed against 6.5L4. Bidirectional arrows with thick edges indicate that each competitor, when initially rare, can invade the other, implying stable coexistence. Unidirectional arrows with thin edges point from superior competitors to losing strains, regardless of the initial ratio. Interior arrows point from initially rare (10% frequency) to initially common (90%) strains, and adjacent values show the fitness of rare relative to common competitors. Values >1 indicate that rare strains could invade common strains; values <1 indicate that rare strains could not invade. Means and 95% confidence intervals are shown in figs. S2 and S3.

at least one more derived allele would be necessary to allow a constructed genotype to invade the L lineage. Mutations in *spoT*, a global regulatory gene, are among the most beneficial in the long-term populations (*16, 22*), and a mutation in *spoT* was fixed before the S and L lineages diverged (table S2). We combined the *spoT*, *arcA*, and *gntR* alleles in the ancestral background, and together they conferred the ability to invade and stably coexist with 6.5L4 (Fig. 1C and fig. S3). Thus, these mutations provide sufficient overall

adaptation and ecological differentiation to allow a constructed S ecotype to coexist with the evolved L ecotype.

When strains containing all possible combinations of the three derived alleles in the ancestral background competed against 6.5L4, we observed complex epistatic interactions (Fig. 2 and fig. S3). The *spoT* mutation increased fitness in all backgrounds, although the magnitude of its benefit varied. The *arcA* mutation was neutral or beneficial, depending on context; the *gntR*

mutation was deleterious or beneficial. Thus, the ability of the S lineage to invade and coexist with the L lineage depended on both the ecological opportunity and synergistic interactions among these mutations.

We also analyzed the individual and joint effects of these three alleles in the ancestral background during competition against the ancestor (*17*). As expected, the derived *spoT* allele was highly beneficial in this context, but neither the *arcA* nor the *gntR* allele was beneficial alone, nor
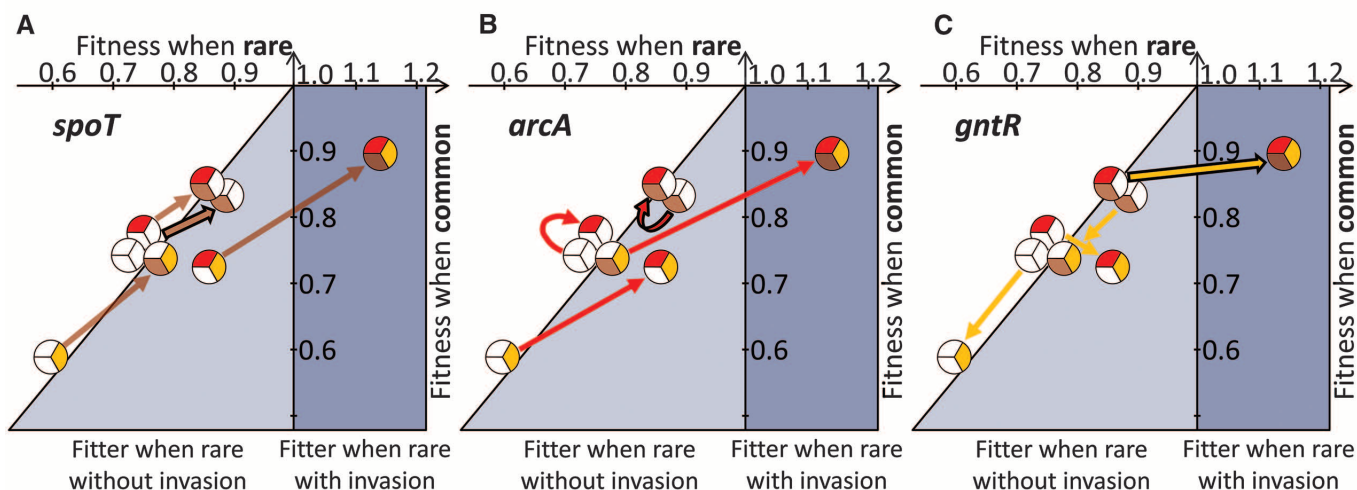
Fig. 2. Interactions among focal mutations. Each panel shows the fitness effects, when rare (*x* axis) and common (*y* axis), of adding the derived (**A**) *spoT*, (**B**) *arcA*, and (**C**) *gntR* allele to various backgrounds in competition with the 6.5L4 clone. Each allele is indicated by a colored sector, as in Fig. 1. The addition of an allele is shown as an arrow pointing away from the genetic background to which it was added. Arrows are colored according to the added allele. Arrows with dark edges show events in the order they occurred during the evolution leading to the S lineage, although other mutations also occurred. The diagonal line represents frequency independence. A circle in the dark region on the right means the strain can invade when rare; circles in the lightly shaded region below the diagonal mean the strains are more fit when rare than when common but cannot invade.
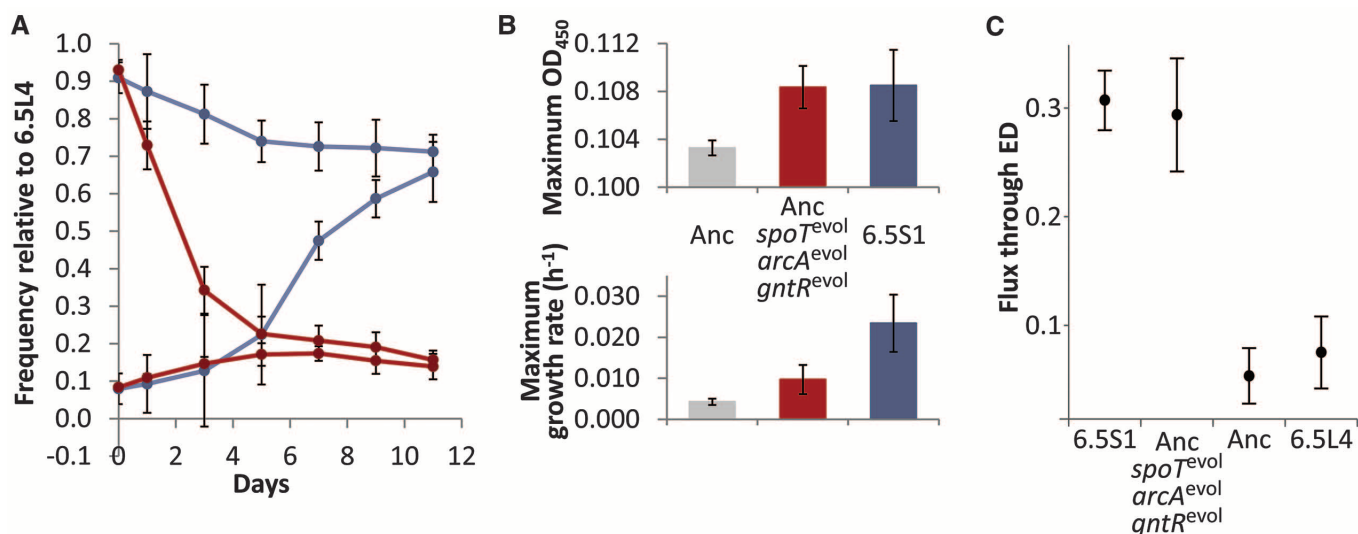
Fig. 3. Phenotypic comparisons of constructed S strain and clone 6.5S1. The constructed S ecotype has the derived *spoT*, *arcA*, and *gntR* alleles in the ancestral background. (**A**) Invasion and coexistence of the constructed S ecotype (red) and clone 6.5S1 (blue) with clone 6.5L4, starting from different initial frequencies. (**B**) Maximum optical density (OD_{450}) and growth rate of the ancestral strain (gray), constructed S strain (red), and 6.5S1 (blue) in the supernatant obtained from a culture where 6.5L4 was previously grown. (**C**) Proportion of glucose flux through the Entner-Doudoroff (ED) pathway for ancestral, evolved, and constructed strains. Error bars in all panels are 95% confidence intervals.
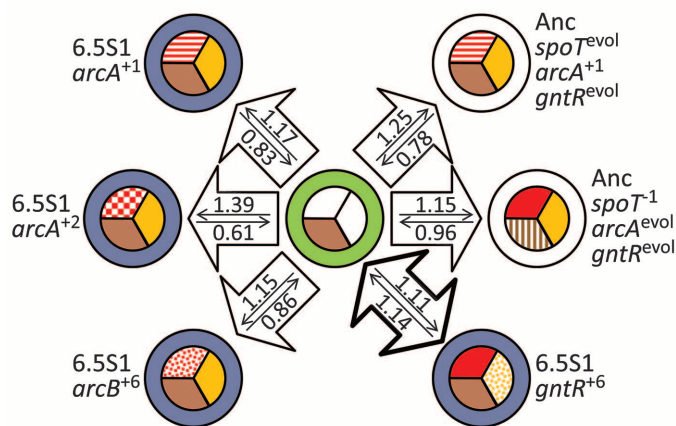
did they increase fitness when combined sequentially with the *spoT* allele (fig. S4A). However, the derived *arcA* and *gntR* alleles were beneficial in the context of the S lineage; replacing either with its ancestral counterpart reduced fitness in competition with clone 6.5S1 (fig. S4B). Therefore, the establishment of the S lineage was a multistep process, with each step dependent on its ecological and genetic context.

We then analyzed the constructed S strain for other phenotypes that characterize the evolved S ecotype (*17*). The constructed S strain stably coexisted with 6.5L4, although with a lower equilibrium density than 6.5S1 (Fig. 3A). The constructed S type also grew faster and reached a higher density on L-conditioned supernatant (*7*) than the ancestor, although its growth rate was slower than 6.5S1 (Fig. 3B). These quantitative differences are unsurprising, however, because 6.5S1 harbors additional beneficial mutations not present in the constructed strain.

The constructed S strain also exhibited changes in central carbon metabolism (*17*), routing ~30% of catabolized glucose through the Entner-Doudoroff pathway rather than glycolysis (Fig. 3C). This flux is similar to that of 6.5S1 and significantly different from the ancestor (*17*). The derived *gntR* allele alone caused a large difference in flux pattern from the ancestor, whereas the *spoT* and *arcA* mutations had only small effects (fig. S5).

More subtle frequency-dependent interactions occur in some other replicate populations (*23*), and one generated an ecotypic polymorphism after evolving the ability to use citrate, an exogenously supplied resource (*4*, *10*). However, Ara–2 appears unique in the strength of its cross-feeding interaction and the persistence of the polymorphism (*7*, *12–14*, *23*). However, many genes show parallel evolution (*16*): *spoT* mutations arose in seven other populations, *arcA* or *arcB* (encoding the regulator and sensor proteins of a two-component system) mutations in 10 others, and a *gntR* mutation in one other (table S6). In fact, one population, Ara+6, has mutations in all three genes.

To explore why Ara–2 followed its atypical evolutionary path, we replaced the *spoT*, *arcA*, and *gntR* alleles found in S with alleles from other populations (*17*) and examined how they affected the ability to invade and coexist with 6.5L4 (Fig. 4 and figs. S6 and S7). With so many alternative alleles, it was not possible to test them all. However, we produced six strains in the constructed S and 6.5S1 backgrounds, where one of the three alleles from S was replaced by an alternative allele from another population. In only one case, the *gntR* allele from Ara+6, did the alternative allele allow invasion of the L ecotype. With a *spoT* allele from Ara-1, the construct could not invade when rare; with four *arcA* and *arcB* replacements, the frequency-dependent interaction was lost and the constructs were less fit than with the S-derived *arcA* allele. Thus, the ecological differentiation and establishment of the S lineage required specific alleles in two genes. These specific mutations were responsible for, in essence, one-half of the stable coexistence of the S and L ecotypes. Other mutations, not yet identified, led to L-specific traits, including the propensity to secrete metabolites, the inability to use the by-products, or both.

In sum, we showed that three mutations, with complex epistatic and frequency-dependent effects, are sufficient to establish one partner in a strong and persistent ecological interaction. All three mutations affect regulators of gene expression, and regulatory changes are important for microbial evolution (*22*, *24*). Other replicate populations fixed mutations in the same genes without evolving such persistent polymorphisms, implying that specific mutations produced qualitatively different evolutionary dynamics. Indeed, allelic exchanges confirm that alternative mutations in these genes preclude coexistence. Thus, a given gene may acquire many potentially beneficial mutations (*16*, *22*, *25*), but subtle variations may determine whether an evolving population remains monotypic or splits into stably coexisting lineages.

References and Notes

1. D. Schluter, *The Ecology of Adaptive Radiations* (Oxford Univ. Press, 2000).
2. J. B. Losos, T. R. Jackman, A. Larson, K. Queiroz, L. Rodriguez-Schettino, *Science* **279**, 2115–2118 (1998).
3. A. J. Spiers, S. G. Kahn, J. Bohannon, M. Travisano, P. B. Rainey, *Genetics* **161**, 33–46 (2002).
4. Z. D. Blount, C. Z. Borland, R. E. Lenski, *Proc. Natl. Acad. Sci. U.S.A.* **105**, 7899–7906 (2008).
5. D. S. Treves, S. Manning, J. Adams, *Mol. Biol. Evol.* **15**, 789–797 (1998).
6. C. C. Spencer, M. Bertrand, M. Travisano, M. Doebeli, *PLOS Genet.* **3**, e15 (2007).
7. D. E. Rozen, R. E. Lenski, *Am. Nat.* **155**, 24–35 (2000).
8. K. N. Laland, F. J. Odling-Smee, M. W. Feldman, *Proc. Natl. Acad. Sci. U.S.A.* **96**, 10242–10247 (1999).
9. M. Doebeli, U. Dieckmann, *Am. Nat.* **156**, (s4), S77–S101 (2000).
10. Z. D. Blount, J. E. Barrick, C. J. Davidson, R. E. Lenski, *Nature* **489**, 513–518 (2012).
11. M. D. Herron, M. Doebeli, *PLOS Biol.* **11**, e1001490 (2013).
12. D. E. Rozen, D. Schneider, R. E. Lenski, *J. Mol. Evol.* **61**, 171–180 (2005).
13. D. E. Rozen, N. Philippe, J. Arjan de Visser, R. E. Lenski, D. Schneider, *Ecol. Lett.* **12**, 34–44 (2009).
14. M. Le Gac, J. Plucain, T. Hindré, R. E. Lenski, D. Schneider, *Proc. Natl. Acad. Sci. U.S.A.* **109**, 9487–9492 (2012).
15. M. J. Wiser, N. Ribeck, R. E. Lenski, *Science* **342**, 1364–1367 (2013).
16. J. E. Barrick *et al.*, *Nature* **461**, 1243–1247 (2009).
17. Materials and methods and supplementary figures and tables are available as supplementary materials on *Science* Online.
18. H. Jeong *et al.*, *J. Mol. Biol.* **394**, 644–652 (2009).
19. P. D. Sniegowski, P. J. Gerrish, R. E. Lenski, *Nature* **387**, 703–705 (1997).
20. R. Malpica, G. R. Sandoval, C. Rodríguez, B. Franco, D. Georgellis, *Antioxid. Redox Signal.* **8**, 781–795 (2006).
21. N. Peekhaus, T. Conway, *J. Bacteriol.* **180**, 3495–3502 (1998).
22. T. F. Cooper, D. E. Rozen, R. E. Lenski, *Proc. Natl. Acad. Sci. U.S.A.* **100**, 1072–1077 (2003).
23. S. F. Elena, R. E. Lenski, *Evolution* **51**, 1058–1067 (1997).
24. T. Hindré, C. Knibbe, G. Beslon, D. Schneider, *Nat. Rev. Microbiol.* **10**, 352–365 (2012).
25. O. Tenaillon *et al.*, *Science* **335**, 457–461 (2012).

Fig. 4. Effects of alternative alleles on ability of S ecotype to invade and coexist with L ecotype. The *spoT* and *arcA* alleles in the constructed S strain were replaced by alternative alleles from populations Ara–1 and Ara+1, respectively. The *arcA* allele in clone 6.5S1 was replaced by alternative alleles from Ara+1 and Ara+2 or by a derived *arcB* allele from Ara+6. The *gntR* allele in 6.5S1 was replaced by an alternative allele from Ara+6. Color schemes for Ara–2–derived alleles and genetic backgrounds, arrows, and fitness values are as in Fig. 1. Alternative alleles from other populations have the same colors as the corresponding Ara–2 alleles, but with hatched or speckled motifs in the corresponding sectors. Means and 95% confidence intervals for each competing pair, along with controls, are shown in fig. S6.